ARTICLE
Journal of Cellular Biochemistry 113:3788–3796 (2012)

Journal of Cellular Biochemistry

Knockdown of Nucleosome Assembly Protein 1-Like 1 Promotes Dimethyl Sulfoxide-Induced Differentiation of P19CL6 Cells Into Cardiomyocytes

Lu Li,[1,2] Hui Gong,[1] Hongxiu Yu,[1] Xiaohui Liu,[1,2] Qingping Liu,[1,2] Guoquan Yan,[1,2] Yang Zhang,[1] Haojie Lu,[1,2] Yunzeng Zou,[1,3]** and Pengyuan Yang[1,2]*

[1]*Institutes of Biomedical Sciences, Fudan University, Shanghai 200032, China*

[2]*Department of Chemistry, Fudan University, Shanghai 200433, China*

[3]*Institutes of Cardiovascular Diseases, Zhongshan Hospital, Fudan University, Shanghai 200032, China*

ABSTRACT

Transplantation of cardiomyocytes derived from stem cells is a promising option for cardiac repair. However, how to obtain efficient cardiomyocytes from stem cells is still a great challenge. Understanding of the mechanism that regulates the cardiac differentiation of stem cells is necessary for the effective induction of cardiomyocytes. A clonal derivative named P19CL6 cells can easily differentiate into cardiomyocytes with 1% dimethyl sulfoxide (DMSO) treatment, which offers a valuable model to study cardiomyocytes differentiation in vitro. In this study, the isobaric tags for relative and absolute quantitation (iTRAQ) proteomics were performed to identify proteins associated with cardiomyocytes differentiation of P19CL6 cells induced by DMSO. Out of 543 non-redundant proteins identified, 207 proteins showed significant changes during differentiation with $\geq$1.2-fold or $\leq$0.83-fold changes cut-offs. Nine proteins were confirmed by the quantitative real-time polymerase chain reaction (qRT-PCR) and Western blot analysis respectively. Notably, broad consistency was well showed between mRNA and protein expression for down-regulation of nucleosome assembly protein 1-like 1 (Nap1l1). Further study revealed that knockdown of Nap1l1 by stable transfection of shRNA vector significantly accelerated DMSO-induced cardiomyocytes differentiation of P19CL6 cells characterized by increases in expression of cardiac specific transcription factors, genes, and proteins (GATA4, MEF-2C, ANP, BNP, cTNT, and β-MHC). Therefore, Nap1l1 is a novel protein that regulates cardiomyocytes differentiation of P19CL6 cells induced by DMSO. J. Cell. Biochem. 113: 3788–3796, 2012.

KEY WORDS: NUCLEOSOME ASSEMBLY PROTEIN 1-LIKE 1; iTRAQ; MASS SPECTROMETRY; CELL DIFFERENTIATION

Cardiovascular disease remains the leading cause of death worldwide. Acute ischemic injury and chronic cardiomyopathies lead to permanent loss of cardiomyocytes and ultimately heart failure. In recent years, cell therapy has emerged as a potential new strategy for patients with ischemic heart disease. Studies in animal models and clinical trials indicated that various stem cell populations have the potential for cardiac repair and regeneration, and improve the function of ventricular muscle after transplanted into the injured heart [Sadek et al., 2009; Liang et al., 2010; Poynter et al., 2011; Templin et al., 2011]. However, the current experimental evidence suggests that low generation of new cardiomyocytes limits the clinic outcomes of stem cell therapy to a great extent. In order to enhance the efficacy of stem cell differentiation into cardiomyocytes, identification of novel proteins or factors associated with differentiation is beneficial to develop new strategies for stem cell therapy in cardiac diseases.

The authors declared that they have no conflicts of interest.

Additional supporting information may be found in the online version of this article.

Grant sponsor: National Basic Research Program of China; Grant number: 2010CB945500; Grant sponsor: Science and Technology Commission of Shanghai Municipality; Grant number: 08dj1400504; Grant sponsor: Doctoral Fund of Ministry of Education of China; Grant number: 200802461124.

*Correspondence to: Pengyuan Yang, Institutes of Biomedical Sciences, Fudan University, Shanghai 200032, China. E-mail: pyyang@fudan.edu.cn

**Correspondence to: Yunzeng Zou, Institutes of Cardiovascular Diseases, Zhongshan Hospital, Fudan University, Shanghai 200032, China. E-mail: zou.yunzeng@zs-hospital.sh.cn

Manuscript Received: 29 February 2012; Manuscript Accepted: 5 July 2012

Accepted manuscript online in Wiley Online Library (wileyonlinelibrary.com): 13 July 2012

DOI 10.1002/jcb.24254 • © 2012 Wiley Periodicals, Inc.

P19CL6 cells, a derivative clone of P19 mouse embryonic carcinoma cells (ECCs), can efficiently differentiate into cardiomyocytes with 1% dimethyl sulfoxide (DMSO) treatment under adherent culture conditions [Habara-Ohkubo, 1996]. Given this unique property, P19CL6 cells are expected as a powerful tool for in vitro differentiation studies of ECCs and therapeutic potential in cardiovascular regenerative medicine. Applying proteomics to investigate the programs that control differentiation will provide valuable insights into how the factors involved induce differentiation of stem cells to specific lineages. Recently, the isobaric tags for relative and absolute quantification (iTRAQ)-based proteomic technique have attracted much attention due to quantifying proteins from different samples in a single experiment. In this research, we employed iTRAQ technology workflow to identify proteins associated with DMSO-induced differentiation of P19CL6 cells into cardiomyocytes. Furthermore, nine of the differentially expressed candidates were validated by qRT-PCR and Western blot analysis. Interestingly, we observed that knockdown of Nap1l1 promoted DMSO-induced differentiation of P19CL6 cells into cardiomyocytes. This work will result in generation of new information and knowledge about research of cardiomyocytes differentiation and cell-therapy for cardiovascular disease.

MATERIALS AND METHODS

CELL CULTURE AND DIFFERENTIATION

P19CL6 cells were kindly provided by Prof. Issei Komuro (Department of Cardiovascular Science and Medicine, Chiba University, Japan). P19CL6 cells were cultured and induced to differentiate into cardiomyocytes essentially as described previously with a slight modification [Habara-Ohkubo, 1996]. Briefly, the cells were grown in α-MEM supplemented with 10% fetal bovine serum, referred as growth medium, and were maintained in a 5% CO_2 atmosphere at 37°C.To induce differentiation, P19CL6 cells were plated at a density of 1.8×10^5 cells in a 35 mm dish or 6.5×10^3 cells per well in 96-well plate with the growth medium containing 1% DMSO (Sigma–Aldrich), referred as differentiation medium, for 8 days, and then the cells were transferred to growth medium for 4 days more. The medium was changed every 2 days. Days of differentiation were numbered consecutively after treatment with DMSO.

IMMUNOFLUORESCENCE

P19CL6 cells treated or not treated with DMSO on Day 12 were fixed with 4% paraformaldehyde in phosphate buffered saline (PBS) at room temperature for 20 min and then permeated with 0.2% Triton X-100 in PBS at room temperature for 15 min. After being blocked with 5% BSA in PBS for 1 h, the cells were incubated with cardiac myosin heavy chain antibody (β-MHC, Abcam) diluted in PBS at a concentration of 1:100 overnight at 4°C, and followed by detection with Cy^{TM}3-conjugated goat anti-mouse antibody (Jackson) diluted in PBS at a concentration of 1:800 at room temperature in dark for 1 h. DAPI (Sigma–Aldrich) was used for nuclear stain. Images were obtained with 200 magnifications using fluorescent microscope (Olympus IX5). The fluorescence area of β-MHC was calculated by Image J software.

SAMPLE PREPARATION AND iTRAQ LABELING

Total protein was extracted from P19CL6 cells on day 0, day 4, day 8, and Day 12 using lysis buffer (8 M urea, 2 M thiourea, 2%CHAPS, 60 mM DTT) containing complete protease inhibitor cocktail (Roche). Protein lysates were then clarified by centrifugation at 4°C at 12,000*g* for 20 min. The protein concentration was determined by the Bradford assay kit (Bio-Rad). A total of 100 μg protein from each group was subjected to six volume of cold acetone precipitation overnight at 4°C before the precipitated pellets were resuspended with dissolution buffer containing 20 μl of 500 mM triethylammonium bicarbonate (TEAB) and 1 μl of 2% SDS. Subsequently, the resuspended proteins were reduced with 2 μl of 50 mM tris-2-carboxyethyl phosphine (TCEP) at 60°C for 1 h and then alkylated with 1 μl of 200 mM methyl methanethiosulfonate (MMTS) in isopropanol at room temperature for 10 min, followed by digestion with 10 μg sequencing grade trypsin (Applied Biosystems) for 16 h at 37°C. The 114, 115, 116, and 117 iTRAQ reagents were dissolved each in 70 μl of ethanol. Peptide samples were labeled with iTRAQ tags at room temperature for 1 h as follows: day0–114tag, day4–115tag, day8–116tag, and day12–117tag. Then all labeled peptides were pooled and dried in a vacuum concentrator prior to SCX fractionation. Two biological samples were prepared and analyzed on separate occasions.

STRONG CATION EXCHANGE FRACTIONATION

The dried mixtures above were reconstituted in 100 μl buffer A (10 mM KH_2PO_4 in 25% acetonitrile, pH 2.7) and fractionated using a Poly Sulfoethyl A Column (2.1 mm × 100 mm, 5 μm, 200 Å, PolyLC, Inc.MA) on a Micro LC-20AD HPLC unit (Shimadzu) with a constant flow rate of 200 μl/min. The 60 min gradient consisted of 100% buffer A for 5 min, 0–25% buffer B (buffer A with 350 mM KCl) for 35 min, 25–100% buffer B for 5 min, and 100% buffer B for 5 min and finally 100% buffer A for 5 min. The chromatogram was monitored through a UV detector which wavelengths were set at 214 nm. Fractions were collected every minute and later pooled together according to variations in UV peak intensity. A total of 20 SCX fractions were collected, vacuumed, and stored at −80°C prior to mass spectrometric analysis.

MASS SPECTROMETRIC ANALYSIS

Each vacuumed fraction was reconstituted in 40 μl of mobile phase A (0.1% formic acid in 5% acetonitrile). The reversed phase liquid chromatograph system consisted of a Michrom Cap Trap^{TM} column (0.5 mm × 2 mm) and an analytical column (Magic C18AQ, 3 μm, 200 Å, 0.1 mm × 150 mm, Michrom BioResources) with a constant flow rate of 0.5 μl/min. The LC gradient started with 5% mobile phase B (0.1% formic acid in 95% acetonitrile) for 5 min, followed by 5–35% mobile phase B for 65 min, then 80% mobile phase B for 5 min, and finally 5% mobile phase B for 10 min. The Q-Star XL Hybrid ESI mass spectrometer (Applied Biosystems) was set to perform data acquisition in information dependent acquisition mode, with a selected mass range of 400–1,800 m/z. Peptides with +2 to +4 charge states were selected for tandem mass spectrometry, and the time of summation of MS/MS events was set to 2 s. The four most abundantly charged peptides above 20 counts threshold were

selected for MS/MS and dynamically excluded for 45 s with ±100 ppm mass tolerance.

DATA ANALYSIS AND INTERPRETATION

For protein identification and quantitation, MS/MS data were analyzed using the ProteinPilot 2.0 software (Applied Biosystems), which applies the Paragon Algorithm [Shilov et al., 2007]. The search was performed against an IPI Mouse 3.55 database and Mouse UniProt Knowledgebase 15.6 database respectively. A concatenated target-decoy database search strategy was also employed to exclude false positives [Elias and Gygi, 2007]. The search parameters allowed for sample type with iTRAQ 4Plex Peptide Labeled, trypsin as the digestion agent, cysteine modification by MMTS, thorough search effort and biological modifications programmed in the algorithm. The bias correction was applied to account for normalization errors. Proteins identified with at least 95% confidence (unused ProtScore ≥1.3) were reported for further analysis. The differentially expressed proteins were classified with biological processes using Gene Ontology classification system [Ashburner et al., 2000; Consortium, 2006]. The protein–protein interaction network was extracted using search tool STRING (version 9.0, http://string-db.org/) [Jensen et al., 2009].

QUANTITATIVE REAL-TIME POLYMERASE CHAIN REACTION

Total cellular RNA was isolated from the cells on day 4, day 8, and Day 12 with the Purelink RNA kit (Invitrogen) according to manual instructions. cDNA was synthesized with the High Capacity cDNA Reverse Transcription kit (Applied Biosystems) according to manual instructions. The quantitative real-time polymerase chain reaction (qRT-PCR) amplification was performed with the Power SYBR Green PCR Master Mix (Applied Biosystems) on a Bio-Rad iQ5 real-time PCR detection system. All primers are listed in Supplemental Table S1. The parameters for amplification are as follows: an initial step of 95°C for 10 min; then 40 cycles of denaturation at 95°C for 15 s, and annealing at 60°C for 1 min. After amplification, melting curve analysis was performed as described in the manufacture's protocol (Bio-Rad). β-actin was selected as an internal control. Data analysis were carried out using the $2^{-\Delta\Delta Ct}$ method. Three biological samples were prepared and the qRT-PCR experiments were repeated by three times for each biological sample.

WESTERN BLOT ANALYSIS

Total protein lysates extracted from the experiments as described above for the LC–MS/MS analysis were used for Western blot analysis. Equal amounts of proteins from each group (day 0, day 4, day 8, and day 12) were separated by 12% SDS–PAGE gel and transferred electrophoretically onto a polyvinylidene difluoride (PVDF) membrane (Millipore). After blocking with 5% BSA in TBST buffer (10 mmol/L Tris, 150 mmol/L NaCl, and 0.1% Tween-20, pH 7.5) for 1 h at room temperature, the PVDF membrane was probed with primary antibody as below in TBST buffer containing 5% BSA overnight at 4°C, followed by horseradish peroxidase-conjugated secondary antibody in TBST for 1 h at room temperature, and developed using the ECL Western blot detection kit (GE Healthcare) according to manual instructions. The following primary antibodies and secondary antibodies were used: nucleosome assembly protein 1-like 1 (Nap1l1, 1:1,000, Abcam), activated RNA polymerase II transcriptional co-activator p15 (Sub1, 1:1,000, Proteintech), heat shock 70 kDa protein 5 (Hspa5, 1:1,000, Abcam), 14-3-3 protein zeta/delta (Ywhaz, 1:1,000, Abcam), superoxide dismutase 1 (Sod1, 1:2,000, Abcam), peroxiredoxin 2 (Prdx2, 1:2,000, Abcam), macrophage migration inhibitory factor (Mif, 1:2,000, Abcam), acidic (leucine-rich) nuclear phosphoprotein 32 family, member A (Anp32a, 1:2,000, Abcam), elongation factor 2 (Eef2, 1:1,000, Cell Signaling Technology), cardiac troponin T (cTNT, 1:1,500, Proteintech), β-actin (1:10,000, KangChen Bio-tech Inc.), goat anti-mouse IgG horseradish peroxidase-conjugated antibody (1:10,000, Sigma–Aldrich), and goat anti-rat IgG horseradish peroxidase-conjugated antibody (1:10,000, Jackson).

TRANSFECTION OF Nap1l1 shRNA TO P19CL6 CELLS

For shRNA-mediated knockdown, pLKO.1-puro vectors targeting for the mouse Nap1l1 gene (NM_015781, Mission TRCN0000092889, Sigma–Aldrich) were transfected into P19CL6 cells with Lipofectamine2000™ reagent (Invitrogen) in accordance with manual instructions. A scrambled non-target shRNA (SHC002, Sigma–Aldrich) was used as control. Stable puromycin-resistant clones (2 μg/ml) were selected for further studies. The Mission TRCN0000092889 was abbreviated as TRCN89 in follow. Nap1l1 expression level was determined by qRT-PCR and Western blot analysis as described above. P19CL6 cells, knockdown of Nap1l1, were cultured, and differentiated for 12 days as described above. Cardiomyocyte differentiation was evaluated by the expression of cardiac specific transcription factors, genes, and proteins (GATA4, MEF-2C, ANP, BNP, cTNT, and β-MHC), which were determined by qRT-PCR, Western blot analysis, and fluorescence area as described above.

STATISTICAL ANALYSIS

The statistical significance of difference was determined by ANOVA or Student's *t*-test with a value of $P < 0.05$. Bar charts were plotted for matched samples with SigmaPlot 10.0 software.

RESULTS

CELL DIFFERENTIATION

Following treatment with growth medium and differentiation medium, the differentiation of P19CL6 cells into cardiomyocytes was characterized by detecting the expression of β-MHC at Day 12 (Fig. 1A) and increases of cardiac specific transcription factors and genes (GATA4, MEF-2C, ANP, and BNP) in the process of differentiation from the qRT-PCR analysis (Fig. 1B). Spontaneously contracting patches of differentiated cardiomyocytes could be easily observed over a period of 12 days with 200 magnifications (Supplemental Video 1). It was suggested that P19CL6 cells successfully and effectively differentiate into cardiomyocytes after treatment with 1% DMSO on day 12.

PROTEIN IDENTIFICATION

Proteomics is proved to be a powerful approach to gain insight into differentiation-associated proteins. In this research, iTRAQ-coupled 2D LC–MS/MS approach was applied to profile proteins in the

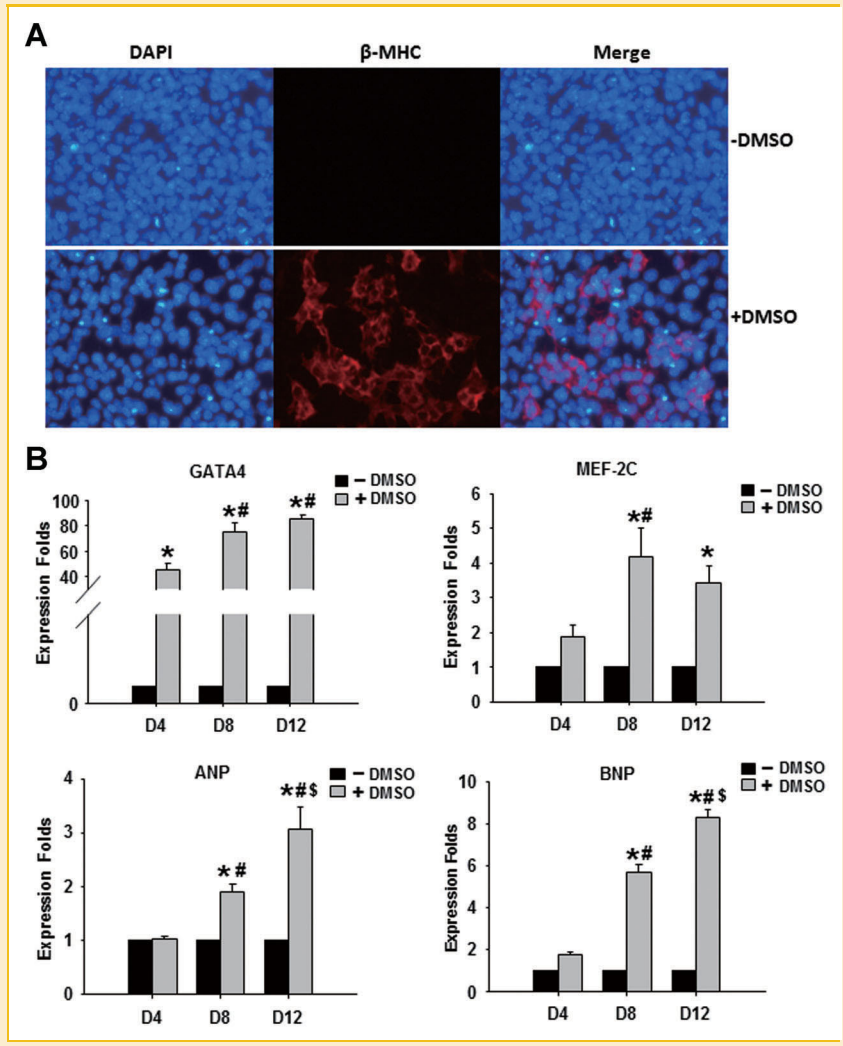

Fig. 1. P19CL6 cells effectively differentiate into cardiomyocytes induced by DMSO. A: Immunofluorescence staining with β-MHC antibody for P19CL6 cells treated (bottom) or not treated (up) with 1% DMSO on day 12. Differentiated cells were stained with β-MHC antibody (Red); Nuclei were counterstained with DAPI (Blue). (×200 magnifications). B: The expression of cardiac specific transcription factors and genes (GATA4, MEF-2C, ANP, and BNP) for P19CL6 cells on day 4, Day 8 and day 12. The relative expression folds were determined by qRT-PCR normalized to β-actin. Error bars show SEM day 4, day 8, and Day 12 with DMSO treatment versus day 4, day 8, and Day 12 without DMSO treatment respectively, $^{*}P < 0.05$; Day 8 and Day 12 with DMSO treatment versus Day 4 with DMSO treatment, $^{\#}P < 0.05$; Day 12 with DMSO treatment versus Day 8 with DMSO treatment, $^{\$}P < 0.05$.

process of differentiation. The experiment was designed as Figure 2A. The unused ProtScore was set to 1.3 to achieve 95% confidence. Relative quantification ratios with statistical analysis (*P*-value) were reported by ProteinPilot 2.0 with Paragon Algorithm. In a few case, some iTRAQ ratios and *P*-values were not available due to insufficient mass spectra information or single peptide assignment. We take an additional 1.2-fold change cut-offs for all iTRAQ ratios, that is, ratio ≥ 1.2 or ratio ≤ 0.83, to classifying proteins as up or down regulation, respectively. The criterion of cut-offs were also accepted by several previous researches [Guo et al., 2007; Datta et al., 2010; Unwin et al., 2010]. Two biological samples were prepared and analyzed on separate occasions. Each occasion was searched against IPI Mouse 3.55 database and Mouse UniProt Knowledgebase 15.6 database respectively. Four batches of data were generated (Supplemental Excel). Therefore, 543 non-redundant proteins were identified (Supplemental Excel). 207 proteins were found to display differential expression at least day 4, day 8, or Day 12 compared to Day 0 (Supplemental Table S2). As a representative, an ESI-derived MS/MS spectrum for one of the iTRAQ-tagged peptides of Nap1l1 was showed in Supplemental Figure S1.

PROTEINS CLASSIFICATION AND NETWORK

Total significant proteins detected by iTRAQ analysis were classified according to their biological processes using Gene Ontology classification system. Detailed information was provided in Figure 2B. The categories were mainly involved in translation, protein folding, regulation of transcription, transport, response to stress, metabolic process, oxidation–reduction process, nucleosome assembly, ribosome biogenesis, RNA splicing, etc. Protein interac-

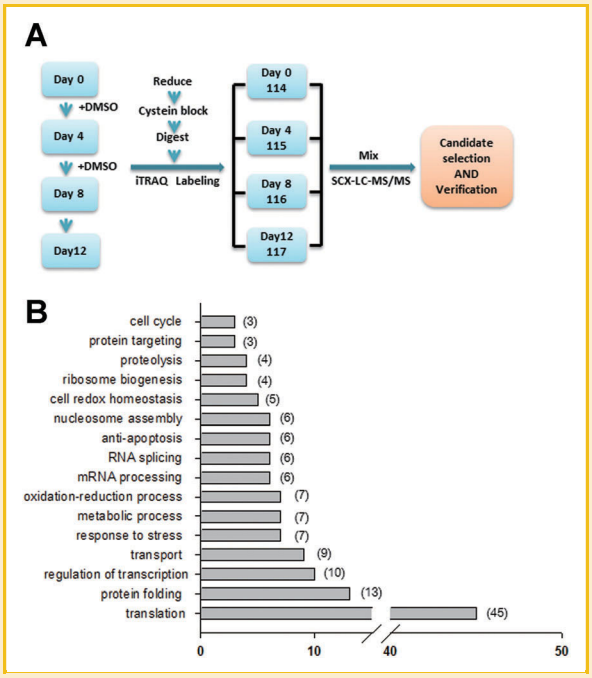

Fig. 2. iTRAQ-coupled protein profiling in the process of P19CL6 cells differentiation into cardiomyocytes. A: Schematic diagram of iTRAQ-coupled 2D LC–MS/MS in P19CL6 cells differentiation into cardiomyocytes with 1% DMSO treatment. Proteins from day 0, day 4, day 8, and Day 12 were reduced with TCEP, blocked with MMTS, digested with trypsin and then labeled with iTRAQ tags respectively (day0–tag114, day4–tag115, day8–tag116, and day12–tag117). All tags were combined followed by SCX-LC–MS/MS analysis. Two biological samples were prepared and analyzed on separate occasions. B: Classification of the differentially expressed proteins identified in the process of P19CL6 cells differentiation into cardiomyocytes. Proteins were categorized with biological processes using Gene Ontology classification system. Since some proteins may be designated with more than one GO assignment, a total of 428 GO assignments were obtained from 207 differentially expressed proteins detected. The main GO assignments were showed above. The numbers in bracket represent the amount of differentially expressed proteins corresponding to each GO assignment. [Color figure can be seen in the online version of this article, available at http://wileyonlinelibrary.com/journal/jcb]

tions among the regulated proteins were explored and an interaction map was created using STRING based on reported protein interaction (Supplemental Fig. S2).

VALIDATION OF DIFFERENTIALLY EXPRESSED PROTEINS

In order to confirm the relative quantitative results from iTRAQ analysis, we performed qRT-PCR and Western blot analysis for the expression of Nap1l1, Sub1, Hspa5, Ywhaz, Sod1, Prdx2, Mif, Anp32a, and Eef2, normalized to β-actin (Fig. 3). The stepwise down-regulation of Nap1l1 mRNA and protein were in line with the results from iTRAQ. Hspa5, Mif, Eef2, and Sod1 showed partial congruence between qRT-PCR and iTRAQ assay. However, Sub1, Ywhaz, Anp32a, and Prdx2 showed discordance between qRT-PCR and iTRAQ assay. The discrepancy between mRNA and protein levels suggests the importance of post-transcription and post-translation during cell differentiation, including post-transcriptional alternative splicing and post-translational protein modification and selective degradation of proteins. On the basis of chemiluminescence intensity measurement, Western blot confirmed the relative quantitative changes observed in iTRAQ approach independently: up-regulated trend for Sub1, Hspa5, Ywhaz, Sod1, Prdx2, Mif, and Anp32a; down-regulated trend for Nap1l1 and Eef2. Since iTRAQ-tagged mass spectrometry and Western blot are approaches based on different technical principle, it is not surprising that the changes are not always exactly coincident. Therefore, those candidates showed the general congruence between antibodies-based and mass spectrometry-based approaches on the whole, which demonstrated that the iTRAQ-coupled 2D LC–MS/MS strategy is an accuracy and effective method for time dependent samples.

KNOCKDOWN OF Nap1l1 PROMOTES DMSO-INDUCED CARDIOMYOCYTES DIFFERENTIATION

In order to verify the effect of Nap1l1 in DMSO-induced differentiation of P19CL6 cells into cardiomyocytes, shRNA vector targeting for Nap1l1 (TRCN89) was stably transfected into P19CL6 cells to silence Nap1l1 gene and a scrambled non-target shRNA was transfected as control. qRT-PCR and Western blot analysis indicated that Nap1l1 expression was reduced by about 80% in P19CL6 cells transfected with TRCN89 vector compared with control group (Fig. 4A,B). Knockdown of Nap1l1 in P19CL6 cells, promoted the expression of cTNT, one of cardiac markers, induced by 1% DMSO at Day 12 (Fig. 4C). However, Nap1l1 deficiency had no effect on the differentiation of P19CL6 cells without DMSO treatment. To prove effective differentiation of cardiomyocytes, especially under the condition of Nap1l1 knockdown, the cardiomyocytes percentage was determined by the fluorescence area of β-MHC. The percentage of β-MHC fluorescence area was enlarged from 30% to nearly 50% with DMSO treatment in the condition of Nap1l1 knockdown. Meanwhile, β-MHC was not detected in either control or TRCN89 group without DMSO treatment (Fig. 4D). Further research revealed that the mRNA expression of cardiac specific transcription factors and genes (GATA4, MEF-2C, ANP, and BNP) were significantly increased by down-regulation of Nap1l1 in P19CL6 cells treated with 1% DMSO (Fig. 4E). Spontaneously contracting patches of differentiated cardiomyocytes were obviously observed at Day 12 with 200 magnifications in P19CL6 cells after knockdown of Nap1l1 treated with 1% DMSO (Supplemental Video 2). Our data indicated that knockdown of Nap1l1 promoted DMSO-induced differentiation of P19CL6 cells into cardiomyocytes.

DISCUSSION

Cardiovascular disease is a leading cause of death in the worldwide. In addition to the treatments of drug administration, coronary stenting, coronary artery bypass grafts, and electrophysiological treatments, cell-based therapy is an emerging and promising field with the rapid development of regenerative medicine. Future researches aimed at disclosure of star molecules and its mechanism of cell therapy for cardiovascular disease will be necessary for the advancement of this field. In this study, P19CL6 cells were used as a model for stem cell differentiation into cardiomyocytes actions in vitro. We have generated a catalog of protein profiles of P19CL6

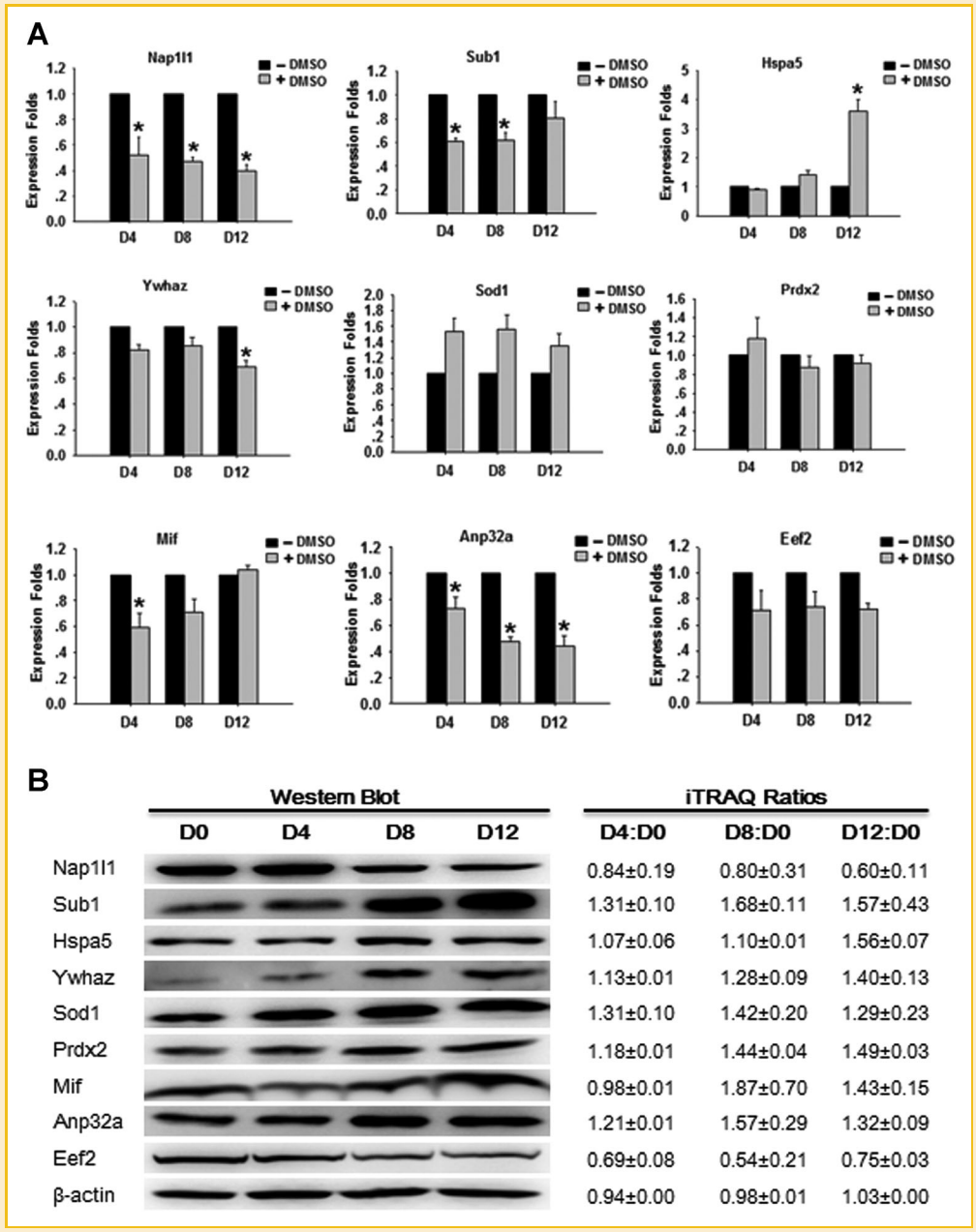

Fig. 3. Validation of differentially expressed proteins detected in P19CL6 cells differentiation process. A: Verification of candidates by qRT-PCR analysis. Total cellular RNA from day 4, day 8, and Day 12 were isolated and subjected to qRT-PCR essay with gene-specific primers, normalized to β-actin. Error bars show SEM day 4, day 8, and Day 12 with DMSO treatment versus day 4, day 8, and Day 12 without DMSO treatment respectively, $^{*}P < 0.05$. B: Verification of candidates by Western blot. The proteins extracted from day 0, day 4, day 8, and day 12, abbreviated as D0, D4, D8, and D12, were separated by SDS–PAGE and then immunoblotted with antibodies against Nap1l1, Sub1, Hspa5, Ywhaz, Sod1, Prdx2, Mif, Anp32a, Eef2, and β-actin to confirm their relative quantitation obtained by iTRAQ. β-actin was selected as an internal control. The iTRAQ ratios of D4:D0, D8:D0, and D12:D0 (115/114, 116/114, and 117/114) showed the relative abundance of proteins in day 4, day 8, and Day 12 compared to day 0, respectively. Two biological samples were prepared and analyzed on separate occasions. Each occasion was searched against IPI Mouse 3.55 database and Mouse UniProt Knowledgebase 15.6 database respectively. Four batches of data were generated (Supplemental Excel). The iTRAQ ratio for the candidates was displayed with mean ± SD.

cells during the differentiation process and documented a total of 207 differentially expressed proteins using iTRAQ-based proteomic approaches. Nap1l1, Sub1, Hspa5, Ywhaz, Sod1, Prdx2, Mif, Anp32a, and Eef2 emerged as interesting candidates and were validated with qRT-PCR and Western blot analysis. Further research indicated that knockdown of Nap1l1 promoted DMSO-induced differentiation of P19CL6 cells into cardiomyocytes. This research firstly revealed that the down-regulation of Nap1l1 may exert a critical role in facilitating stem cell differentiation into cardiomyocytes.

Since the discovery of the nucleosome assembly protein 1 (NAP1) in Laskey et al. [1978], the role of NAP1 orthologous has been

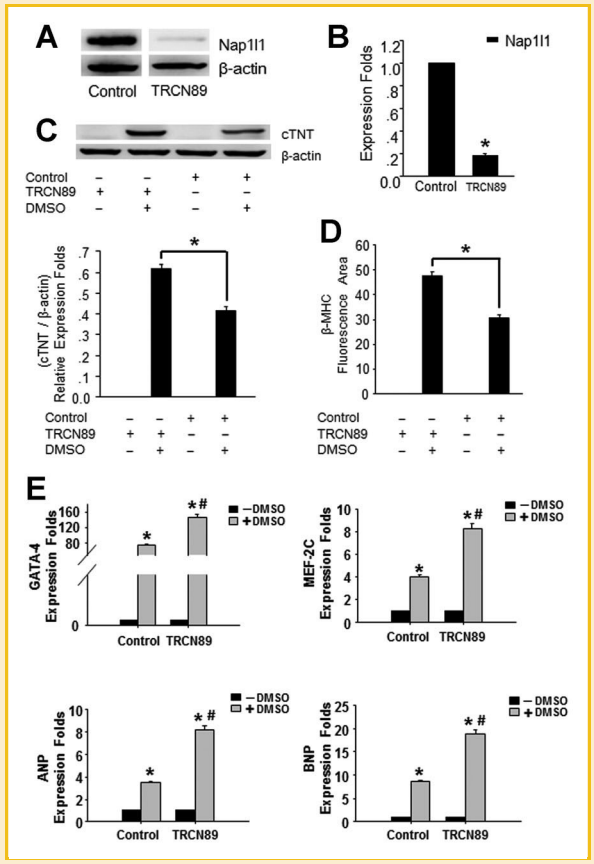

Fig. 4. Knockdown of Nap1l1 promoted DMSO-induced differentiation of P19CL6 cells into cardiomyocytes. A: TRCN89 vectors restrained Nap1l1 protein expression of P19CL6 cells by immunoblot normalized to β-actin. B: TRCN89 vectors repressed Nap1l1 gene expression of P19CL6 cells. The relative expression folds were determined by qRT-PCR normalized to β-actin. Error bars show SEM. TRCN89 versus control, $^{*}P < 0.05$. C: Knockdown of Nap1l1 promoted cTNT expression, a cardiac marker, with 1% DMSO treatment ($^{*}P < 0.05$). Control or TRCN89 transfected only have no effect on cTNT expression without DMSO treatment. D: The cardiomyocytes percentage was determined by the fluorescence area of β-MHC. The percentage of β-MHC fluorescence area was enlarged from 30% to nearly 50% with DMSO treatment in the condition of Nap1l1 knockdown. Meanwhile, β-MHC was not detected in either control or TRCN89 group without DMSO treatment. E: Knockdown of Nap1l1 promoted cardiac specific transcription factors and genes expression, GATA4, MEF-2C, ANP, and BNP, in treatment with 1% DMSO. The relative expression folds were determined by qRT-PCR normalized to β-actin. Error bars show SEM. Control with DMSO treatment versus control without DMSO treatment, $^{*}P < 0.05$; TRCN89 with DMSO treatment versus TRCN89 without DMSO treatment, $^{*}P < 0.05$; TRCN89 with DMSO treatment versus control with DMSO treatment, $^{\#}P < 0.05$.

studied in a variety of eukaryotic species. NAP1 family members share a structurally conserved fold, the NAP domain. Although NAP1 was initially identified as histone chaperones and chromatin-assembly factors, additional functions include roles in tissue-specific transcription regulation, histone shuttling, apoptosis, and cell-cycle regulation [Park and Luger, 2006; Zlatanova et al., 2007; Attia et al., 2011]. In humans and mice, NAP1 gene family consists of at least five members, Nap1l1, Nap1l2, Nap1l3, Nap1l4, and Nap1l5. An interesting finding is that three of NAP1-like proteins (Nap1l2, Nap1l3, and Nap1l5) are expressed exclusively or predominantly in brain [Rougeulle and Avner, 1996; Watanabe et al., 1996; Shen et al., 2001; Smith et al., 2003]. However, Nap1l1 and Nap1l4 are expressed ubiquitously in all vertebrates. Some publications described Nap1l1 as a cancer-related protein [Al-Dhaheri et al., 2006; Kidd et al., 2006; Drozdov et al., 2009]. Diacylglycerol kinase (DGK) is involved in the regulation of lipid-mediated signal transduction through the metabolism of a second messenger diacylglycerol. Nap1l1 and Nap1l4 serve as a cytoplasmic anchor of DGKζ and have a potential protective effect against stressed conditions. The molecular interaction of DGKζ, Nap1l1, and Nap1l4 affects the subcellular localization of DGKζ: Nap1l1 and Nap1l4 prohibit nuclear import of DGKζ by blocking its interaction with import carrier proteins. Furthermore, overexpression of Nap1l1 and Nap1l4 exerts a protective effect against doxorubicin-induced cytotoxicity [Okada et al., 2011]. Nap1l1 are mainly located in nucleus and melanosome. It participates in DNA replication and biological process of nucleosome assembly, which indicates that Nap1l1 play an important role in modulating chromatin formation and contribute to the regulation of cell proliferation. Two-hybrid analysis has revealed a strong interaction of Nap1l1 and Nap1l4 proteins with neuron-specific Nap1l2 protein [Attia et al., 2011]. Nap1l2 likely represents a class of tissue-specific factors interacting with chromatin to regulate neuronal cell proliferation. The murine Nap1l2 gene has been indicated to play an essential role in neural tube development and neuronal differentiation [Rogner et al., 2000]. Nap1l2 regulates transcription in developing neurons via the control of histone acetylation [Attia et al., 2007]. There is also evidence that zygotic Xenopus nucleosome assembly protein-like 1 has a specific, non-cell autonomous role in hematopoiesis [Lankenau et al., 2003]. Repressing alternative differentiation pathways may be important for pluripotent cells to become a specific lineage. Since P19CL6 cells are capable of differentiating into neurons upon stimulation with retinoic acid and into cardiomyocytes upon stimulation with DMSO [Habara-Ohkubo, 1996; Peng et al., 2002], it is reasonable to assume that inhibition of the neural pathway may be important for these cells to develop a cardiac fate. However, there are few reports concerning the role of Nap1l1 in stem cell differentiation, especially in cardiomyocytes differentiation. Thus, our research indicated that knockdown of Nap1l1 promoted the expression of cardiac special transcription factor, genes and proteins in P19CL6 cells induced by DMSO. Further research aimed at elucidating the biological roles and mechanisms of Nap1l1 during cell differentiation in vivo or in vitro seems particularly important and significant.

Hspa5, alternatively named 78 kDa glucose-regulated protein (GRP78), presents multifaceted subcellular position and participates in several biological process: when endoplasmic reticulum retention, it acts as the switch of unfolded protein response; when cell surface residing, it recognizes, and transduces extracellular ligands and signals [Zhang and Zhang, 2010]. During early heart organogenesis, GRP78 can be activated through cooperation between the cell type-specific transcription factors (GATA4) and endoplasmic reticulum stress response element binding factors (ATF6 and YY1) [Russell, 1998; Mao et al., 2006]. Consistency with their results, our results also showed that the expression of Hspa5 increased in differentiated P19CL6 cells. Its particular role in cardiomyogenesis needs further investigation. Anp32a is one

mammalian member of three highly conserved acidic nuclear phosphoprotein 32 kDa families of gene products (Anp32a, Anp32b, and Anp32e) and has been implicated in a broad array of proliferation, differentiation, apoptosis, suppression of transformation, and inhibition of acetyltransferases [Cvetanovic et al., 2007]. There is a hierarchy of Anp32 family proteins function in which Anp32b is the most important family member for embryogenesis, with Anp32a being of moderate importance and Anp32e being of the least importance [Reilly et al., 2011]. Our results showed that Anp32a was highly expressed in differentiated P19CL6 cells. Notably, Anp32b was also detected in the differentiation process, and have a transient increase in early stages (Supplemental Table S2). Therefore, we reasonably speculated that Anp32a participated in the control of P19CL6 cells differentiation. The 14-3-3 protein isoforms act as an adapter protein and interact with signaling molecules including protein kinase C to mediate a wide variety of cellular events such as cell cycle regulation, cell growth and differentiation, anti-apoptosis, and synaptic transmission [Russell, 1998; Skoulakis and Davis, 1998; Fu et al., 2000]. The expression level of 14-3-3 epsilon and Raf-1 is found to be regulated coordinately during rat heart development [Luk et al., 1998]. 14-3-3 eta may play a possible role in growth and differentiation of neurons and astrocytes, and govern coordinated and well-controlled developmental events in the brain to ensure normal neural functions [Chen et al., 2005]. Similarly, our results found that 14-3-3 zeta, theta and beta was richly located in differentiated P19CL6 cells, which allowed further studies to focus on those 14-3-3 protein isoforms and their mechanisms in cell differentiation. Macrophage Mif, discovered as a cytokine inhibited the random migration of macrophages, plays versatile roles in the immune system. Recently, Mif has been reported to be involved in embryonic development in higher vertebrates, such as nervous and sensory systems, and it functions as a growth factor for the proliferation and differentiation of embryonic tissues [Ito et al., 2008; Shen et al., 2012]. Interestingly, Mif is also associated with adipocyte biology during adipogenesis and it regulates differentiation of 3T3-L1 preadipocytes, at least partially, through inhibition of mitotic clonal expansion and/or C/EBPδ expression [Ikeda et al., 2008]. Similarly, we discovered that the expression of Mif increased with the process of P19CL6 cells differentiation. It is worthy of further research, especially the mechanism of participation in regulation of cardiomyogenesis.

Restoring damaged heart tissue, through stem cell repair or regeneration, is a potentially new and promising strategy to treat heart failure, myocardial infarction and various other cardiovascular diseases. Many types of the stem cells, including side population cells, mescenchymal stem cells, endothelial progenitor cells, and cord stem cell, have been reported to make the effect of cell therapy for cardiovascular disease [Sumi et al., 2007; Sadek et al., 2009; Gopinath et al., 2010; Poynter et al., 2011]. A crucial issue in designing more rational cell-based therapy approaches for cardiovascular disease is understanding the mechanisms by which each of the stem cell or progenitor cell types can affect myocardial performance. It should be alerted that potential side effects associated with cell therapy including arrhythmogenesis, tumorigenesis, myocardial injury, infection, and immunologic responses.

In conclusion, this research has characterized changes in proteome pattern of P19CL6 cells differentiation into cardiomyocytes induced by DMSO. Using the iTRAQ shot-gun proteomics, 543 non-redundant proteins were identified. Among them, 207 proteins showed differential expression in the differentiation process. Spotlight was focused on a remarkable change, Nap1l1, involved in nucleosome assembly. Our results suggest that knockdown of Nap1l1 promotes DMSO-induced differentiation of P19CL6 cells into cardiomyocytes. Therefore, further studies aimed at elucidating the biological roles and mechanisms of Nap1l1 in vivo or in vitro will provide more important insights into P19CL6 cells differentiation and effective therapy strategies for cardiovascular disease.

REFERENCES

Al-Dhaheri MH, Shah YM, Basrur V, Pind S, Rowan BG. 2006. Identification of novel proteins induced by estradiol, 4-hydroxytamoxifen and acolbifene in T47D breast cancer cells. Steroids 71:966–978.

Ashburner M, Ball CA, Blake JA, Botstein D, Butler H, Cherry JM, Davis AP, Dolinski K, Dwight SS, Eppig JT, Harris MA, Hill DP, Issel-Tarver L, Kasarskis A, Lewis S, Matese JC, Richardson JE, Ringwald M, Rubin GM, Sherlock G. 2000. Gene ontology: Tool for the unification of biology. The gene ontology consortium. Nat Genet 25:25–29.

Attia M, Rachez C, De Pauw A, Avner P, Rogner UC. 2007. Nap1l2 promotes histone acetylation activity during neuronal differentiation. Mol Cell Biol 27:6093–6102.

Attia M, Forster A, Rachez C, Freemont P, Avner P, Rogner UC. 2011. Interaction between nucleosome assembly protein 1-like family members. J Mol Biol 407:647–660.

Chen XQ, Liu S, Qin LY, Wang CR, Fung YW, Yu AC. 2005. Selective regulation of 14-3-3eta in primary culture of cerebral cortical neurons and astrocytes during development. J Neurosci Res 79:114–118.

Consortium GO. 2006. The Gene Ontology (GO) project in 2006. Nucleic Acids Res 34:D322–D326.

Cvetanovic M, Rooney RJ, Garcia JJ, Toporovskaya N, Zoghbi HY, Opal P. 2007. The role of LANP and ataxin 1 in E4F-mediated transcriptional repression. EMBO Rep 8:671–677.

Datta A, Park JE, Li X, Zhang H, Ho ZS, Heese K, Lim SK, Tam JP, Sze SK. 2010. Phenotyping of an in vitro model of ischemic penumbra by iTRAQ-based shotgun quantitative proteomics. J Proteome Res 9:472–484.

Drozdov I, Kidd M, Nadler B, Camp RL, Mane SM, Hauso O, Gustafsson BI, Modlin IM. 2009. Predicting neuroendocrine tumor (carcinoid) neoplasia using gene expression profiling and supervised machine learning. Cancer 115:1638–1650.

Elias JE, Gygi SP. 2007. Target-decoy search strategy for increased confidence in large-scale protein identifications by mass spectrometry. Nat Methods 4:207–214.

Fu H, Subramanian RR, Masters SC. 2000. 14-3-3 proteins: Structure, function, and regulation. Annu Rev Pharmacol Toxicol 40:617–647.

Gopinath S, Vanamala SK, Gondi CS, Rao JS. 2010. Human umbilical cord blood derived stem cells repair doxorubicin-induced pathological cardiac hypertrophy in mice. Biochem Biophys Res Commun 395:367–372.

Guo Y, Singleton PA, Rowshan A, Gucek M, Cole RN, Graham DR, Van Eyk JE, Garcia JG. 2007. Quantitative proteomics analysis of human endothelial cell membrane rafts: Evidence of MARCKS and MRP regulation in the sphingosine 1-phosphate-induced barrier enhancement. Mol Cell Proteomics 6:689–696.

Habara-Ohkubo A. 1996. Differentiation of beating cardiac muscle cells from a derivative of P19 embryonal carcinoma cells. Cell Struct Funct 21:101–110.

Ikeda D, Sakaue S, Kamigaki M, Ohira H, Itoh N, Ohtsuka Y, Tsujino I, Nishimura M. 2008. Knockdown of macrophage migration inhibitory factor disrupts adipogenesis in 3T3-L1 cells. Endocrinology 149:6037–6042.

Ito K, Yoshiura Y, Ototake M, Nakanishi T. 2008. Macrophage migration inhibitory factor (MIF) is essential for development of zebrafish, Danio rerio. Dev Comp Immunol 32:664–672.

Jensen LJ, Kuhn M, Stark M, Chaffron S, Creevey C, Muller J, Doerks T, Julien P, Roth A, Simonovic M, Bork P, von Mering C. 2009. STRING 8––A global view on proteins and their functional interactions in 630 organisms. Nucleic Acids Res 37:D412–D416.

Kidd M, Modlin IM, Mane SM, Camp RL, Eick G, Latich I. 2006. The role of genetic markers—NAP1L1, MAGE-D2, and MTA1—in defining small-intestinal carcinoid neoplasia. Ann Surg Oncol 13:253–262.

Lankenau S, Barnickel T, Marhold J, Lyko F, Mechler BM, Lankenau DH. 2003. Knockout targeting of the Drosophila nap1 gene and examination of DNA repair tracts in the recombination products. Genetics 163:611–623.

Laskey RA, Honda BM, Mills AD, Finch JT. 1978. Nucleosomes are assembled by an acidic protein which binds histones and transfers them to DNA. Nature 275:416–420.

Liang SX, Tan TY, Gaudry L, Chong B. 2010. Differentiation and migration of Sca1+/CD31- cardiac side population cells in a murine myocardial ischemic model. Int J Cardiol 138:40–49.

Luk SC, Ngai SM, Tsui SK, Chan KK, Fung KP, Lee CY, Waye MM. 1998. Developmental regulation of 14-3-3 epsilon isoform in rat heart. J Cell Biochem 68:195–199.

Mao C, Tai WC, Bai Y, Poizat C, Lee AS. 2006. In vivo regulation of Grp78/BiP transcription in the embryonic heart: Role of the endoplasmic reticulum stress response element and GATA-4. J Biol Chem 281:8877–8887.

Okada M, Hozumi Y, Ichimura T, Tanaka T, Hasegawa H, Yamamoto M, Takahashi N, Iseki K, Yagisawa H, Shinkawa T, Isobe T, Goto K. 2011. Interaction of nucleosome assembly proteins abolishes nuclear localization of DGKzeta by attenuating its association with importins. Exp Cell Res 317:2853–2863.

Park YJ, Luger K. 2006. Structure and function of nucleosome assembly proteins. Biochem Cell Biol 84:549–558.

Peng CF, Wei Y, Levsky JM, McDonald TV, Childs G, Kitsis RN. 2002. Microarray analysis of global changes in gene expression during cardiac myocyte differentiation. Physiol Genomics 9:145–155.

Poynter JA, Herrmann JL, Manukyan MC, Wang Y, Abarbanell AM, Weil BR, Brewster BD, Meldrum DR. 2011. Intracoronary mesenchymal stem cells promote postischemic myocardial functional recovery, decrease inflammation, and reduce apoptosis via a signal transducer and activator of transcription 3 mechanism. J Am Coll Surg 213:253–260.

Reilly PT, Afzal S, Gorrini C, Lui K, Bukhman YV, Wakeham A, Haight J, Ling TW, Cheung CC, Elia AJ, Turner PV, Mak TW. 2011. Acidic nuclear phosphoprotein 32 kDa (ANP32)B-deficient mouse reveals a hierarchy of ANP32 importance in mammalian development. Proc Natl Acad Sci U S A 108:10243–10248.

Rogner UC, Spyropoulos DD, Le Novere N, Changeux JP, Avner P. 2000. Control of neurulation by the nucleosome assembly protein-1-like 2. Nat Genet 25:431–435.

Rougeulle C, Avner P. 1996. Cloning and characterization of a murine brain specific gene Bpx and its human homologue lying within the Xic candidate region. Hum Mol Genet 5:41–49.

Russell P. 1998. Checkpoints on the road to mitosis. Trends Biochem Sci 23:399–402.

Sadek HA, Martin CM, Latif SS, Garry MG, Garry DJ. 2009. Bone-marrow-derived side population cells for myocardial regeneration. J Cardiovasc Transl Res 2:173–181.

Shen HH, Huang AM, Hoheisel J, Tsai SF. 2001. Identification and characterization of a SET/NAP protein encoded by a brain-specific gene, MB20. Genomics 71:21–33.

Shen YC, Thompson DL, Kuah MK, Wong KL, Wu KL, Linn SA, Jewett EM, Shu-Chien AC, Barald KF. 2012. The cytokine macrophage migration inhibitory factor (MIF) acts as a neurotrophin in the developing inner ear of the zebrafish, Danio rerio. Dev Biol 363:84–94.

Shilov IV, Seymour SL, Patel AA, Loboda A, Tang WH, Keating SP, Hunter CL, Nuwaysir LM, Schaeffer DA. 2007. The Paragon Algorithm, a next generation search engine that uses sequence temperature values and feature probabilities to identify peptides from tandem mass spectra. Mol Cell Proteomics 6:1638–1655.

Skoulakis EM, Davis RL. 1998. 14-3-3 proteins in neuronal development and function. Mol Neurobiol 16:269–284.

Smith RJ, Dean W, Konfortova G, Kelsey G. 2003. Identification of novel imprinted genes in a genome-wide screen for maternal methylation. Genome Res 13:558–569.

Sumi M, Sata M, Miura S, Rye KA, Toya N, Kanaoka Y, Yanaga K, Ohki T, Saku K, Nagai R. 2007. Reconstituted high-density lipoprotein stimulates differentiation of endothelial progenitor cells and enhances ischemia-induced angiogenesis. Arterioscler Thromb Vasc Biol 27:813–818.

Templin C, Luscher TF, Landmesser U. 2011. Cell-based cardiovascular repair and regeneration in acute myocardial infarction and chronic ischemic cardiomyopathy-current status and future developments. Int J Dev Biol 55:407–417.

Unwin RD, Griffiths JR, Whetton AD. 2010. Simultaneous analysis of relative protein expression levels across multiple samples using iTRAQ isobaric tags with 2D nano LC-MS/MS. Nat Protoc 5:1574–1582.

Watanabe TK, Fujiwara T, Nakamura Y, Hirai Y, Maekawa H, Takahashi E. 1996. Cloning, expression pattern and mapping to Xq of NAP1L3, a gene encoding a peptide homologous to human and yeast nucleosome assembly proteins. Cytogenet Cell Genet 74:281–285.

Zhang LH, Zhang X. 2010. Roles of GRP78 in physiology and cancer. J Cell Biochem 110:1299–1305.

Zlatanova J, Seebart C, Tomschik M. 2007. Nap1: Taking a closer look at a juggler protein of extraordinary skills. FASEB J 21:1294–1310.